HEAT TRANSFER ENHANCEMENT OF SWIRLING FLOW IN A CIRCULAR PIPE IN THE TRANSITION REGIME

Hajime Nakamura
Department of Mechanical Engineering
National Defense Academy of Japan
1-10-20 Hashirimizu, Yokosuka, Kanagawa, Japan
nhajime@nda.ac.jp

Yoshinori Sugawara
Graduate School of Science and Engineering
National Defense Academy of Japan
1-10-20 Hashirimizu, Yokosuka, Kanagawa, Japan

Shunsuke Yamada
Department of Mechanical Engineering
National Defense Academy of Japan
1-10-20 Hashirimizu, Yokosuka, Kanagawa, Japan
yamadas@nda.ac.jp

Yuki Funami
Department of Mechanical Engineering
National Defense Academy of Japan
1-10-20 Hashirimizu, Yokosuka, Kanagawa, Japan
funami@nda.ac.jp

ABSTRACT

Experiments were conducted focusing on the heat transfer enhancement of a swirling pipe flow in the bulk Reynolds number Re = 1000 ~ 12000, including the transition regime. Measurements were performed downstream of the swirl generator composed of a twisted tape to eliminate the turbulence caused by the insert and focus only on the effect of flow swirling. The spatiotemporal variation of the heat transfer, which was reflected by the flow field near the wall, was measured by high-speed infrared imaging technique. In addition, change in the flow field was measured by laser Doppler velocimetry. By applying the swirl to the flow, the heat transfer coefficient increased against the wall shear stress. In particular, it increased up to 30% at $Re \approx$ 1500 ~ 2000. In the turbulent regime, the turbulent streaky structure in the spatiotemporal heat transfer inclined in the swirling direction. The mean streak spacing became narrower due to the increase in the shear velocity, while the non-dimensional spacing by the wall parameters did not change significantly with the flow swirling. In the laminar regime, the inclined streaky structure, which fluctuated with time, appeared in the spatiotemporal heat transfer by swirling the flow. This is considered to be caused by the flow instability due to the flow swirling, which leads to a large heat transfer enhancement in this regime.

INTRODUCTION

It is well known that flow swirling in a pipe improves heat transfer compared to the pressure drop penalty. (Lopina and Bergles, 1969, Sheikholeslami, et at., 2015, among others). Therefore, swirl generators such as twisted tapes or spiral grooves are often installed in pipelines to enhance the heat transfer in such as heat exchangers. However, the mechanism of the heat transfer enhancement has not been well understood since the swirling flow becomes a very complicated nature in which centrifugal instability acts on the wall turbulence.

In this study, experiments were conducted focusing on the heat transfer enhancement of a swirling pipe flow. Previous studies have suggested that the flow swirling enhances the heat transfer with increasing Reynolds number in the laminar regime (Date, 1974; Manglik and Bergles, 1993a), whereas it is enhanced with decreasing Reynolds number in the turbulent regime (Koch, 1968; Manglik and Bergles, 1993b; Eiamsa-ard et al. 2010). Therefore, in this study, experiments were conducted from the laminar and turbulent regimes including the transition regime.

Measurements were performed *downstream* of the swirl generator (a twisted tape was used in this experiment) to eliminate the turbulence caused by the insert and focus only on the effect of flow swirling. The spatiotemporal variation of the heat transfer, which was reflected by the flow field near the wall, was measured by high-speed infrared imaging technique (Nakamura, 2007), and investigated the change in the thermal streaks when the flow was swirled. In addition, change in the flow field in the pipe was measured by laser Doppler

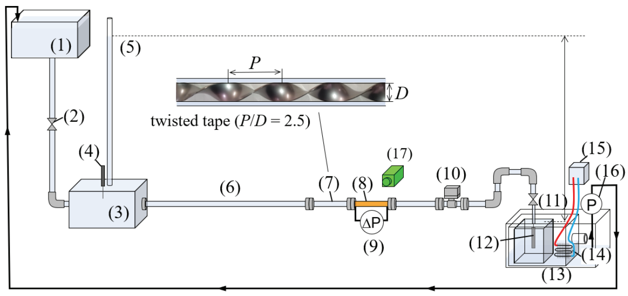

(1) Head tank
(2)(11)Valve
(3) Rectifier tank
(4)(12) Temp. probe
(5) Header
(6) Inlet section
(7) Swirl generator
(8) Test section
(9) Differential manometer
(10) Magnetic flowmeter
(13) Outlet tank
(14) Heat exchanger
(15) Constant temperature water circulator
(16) Pump
(17) Infrared thermograph /Laser Doppler velocimeter

Figure 1. Experimental setup and swirl generator.

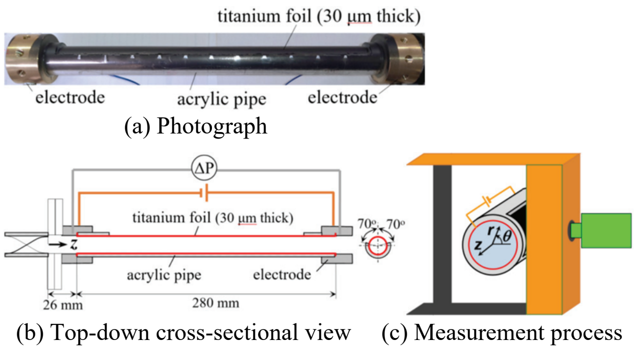

Figure 2. Test section for heat transfer measurements.

velocimetry (LDV) to consider the mechanism that causes the heat transfer enhancement.

EXPERIMENTS

Figure 1 shows the experimental setup that drives the water flow in a horizontal circular pipe by the head difference. The inner diameter of the circular pipe was D = 20 mm and the mean flow velocity ranged from U_m = 0.05 to 0.5 m/s, resulting in the bulk Reynolds number ranged Re = 1000 ~ 12000. The flow in the pipe was swirled by a twisted tape with a length of 200 mm and a width of 20 mm, which was installed behind the inlet section of about 2 m. The twist pitch (length of 180° twist) was P/D = 2.5, 3.3 or 5, whose velocity ratio U_θ/U_m calculated from $(\pi/2)/(P/D)$ were respectively 0.63, 0.47, or 0.31, where U_θ is mean azimuthal velocity.

Figure 2 shows the test section for the heat transfer measurements. The circular duct was fabricated from an acrylic pipe of 280 mm in length (located from z/D = 1.3 to 15.3, z is the streamwise coordinate starting from the twisted tape exit). Titanium foil with a thickness of 30 μm was glued around the entire circumference of the inner surface of the pipe, including the excised section of the pipe. The temperature fluctuation corresponding to the flow turbulence that appeared when the titanium foil was heated electrically was measured by high-speed infrared thermography, as shown in Fig. 2 (c). Simultaneously, the pressure loss Δp between the inlet and outlet of the test section was measured by a high-sensitivity differential manometer.

Time series data of instantaneous temperature distribution measured here, T_w, were used to calculate the spatiotemporal heat transfer coefficient h, considering convection and radiation losses to outside the pipe, thermal diffusion in the heated surface, and thermal inertia of the heated surface (Nakamura et al., 2017). The mean heat transfer coefficient h_m was evaluated from the spatiotemporal averaged values of convective heat flux q_{cv} and temperature difference $T_w - T_m$ (T_m is mixed-mean temperature).

For the velocity measurement, a quartz glass test pipe with a water jacket was used instead of the test model shown in Fig. 2. A biaxial LDV was used to measure the distributions of mean and fluctuating velocities in the pipe. The streamwise velocity u_z and the radial (wall-normal) velocity u_r were measured by the vertical traverse, and the azimuthal velocity u_θ was measured by the horizontal traverse of the pipe cross section. Here, the velocity u is expressed as the sum of the mean velocity U and the fluctuation velocity u'. Since the refractive indexes of water and quartz are different, the traverse coordinates were adjusted to prevent distortion of the measured coordinates.

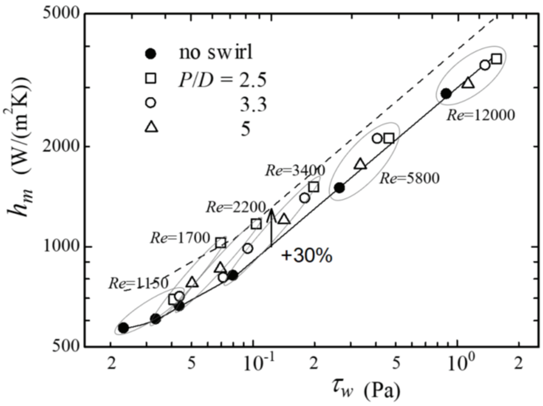

Figure 3. Heat transfer enhancement against wall shear stress.

RESULTS

Heat Transfer Enhancement

The pipe friction coefficient $\lambda = (\Delta p/\Delta z)D/(0.5\rho U_m^2)$ and the mean heat transfer coefficient h_m measured in the absence of the twisted tape reasonably agreed with the well-known empirical formulas in both the turbulent ($Re \geq 5000$) and laminar ($Re \leq 2200$) regimes. Figure 3 shows the mean heat transfer coefficient against the wall shear stress $\tau_w = (\Delta p/\Delta z)D/4$. When the flow is swirled, the heat transfer coefficient increases at the same wall shear stress. In particular, it shows that the heat transfer is largely enhanced at around $Re \approx 2000$ (up to 30% at the same wall shear stress τ_w).

Spatiotemporal Heat Transfer

Figures 4, 5, 6 and 7 show contours of instantaneous heat transfer coefficient at Re = 12000, 5800, 2200 and 1700, respectively. The upper contours of each figure show the case without the twisted tape, and the lower show the case with P/D = 2.5 twisted tape installed.

In the turbulent regime (Figs. 4 and 5), the structure corresponds to the well-known turbulent streaks appears without the twisted tape. In contrast, the streaky structure inclines in the swirling direction when the flow is swirled. The spacing between adjacent streaks becomes narrower by giving the swirl, which increases the heat transfer coefficient. This is mainly because the velocity distribution changes due to the centrifugal force, which increases the shear velocity u_τ (see Fig. 9 (a): velocity gradient at the wall increases due to the swirling). Figure 8 shows the mean spacing of thermal streaks l_c^+ evaluated from the pre-multiplied spectrum of h distribution vertical to the streaks. The superscript '+' indicates the non-dimensional value with the wall parameters (u_τ and kinematic viscosity ν). The non-dimensional streak spacing does not change significantly with the flow swirling to maintain the spacing of about $l_c^+ \approx 100$. This means that the characteristics of wall turbulence are maintained even when the flow is swirled, although the boundary layer becomes thinner and the shear velocity increases. Incidentally, the non-dimensional streak spacing seems to be reduced at $Re \approx 5000$ when the flow is swirled. This is likely to be related to the formation of clearer thermal streaks due to swirling at Re ≈ 5000 (see Fig. 5).

It is interesting to note that the inclination angle of the streaks at $z/D \approx 4$ (about 30° on average, see Fig. 5 (b) at Re = 5800) is larger than the flow inclination angle estimated by $U_\theta/U_z \approx 0.33$ as shown in Fig. 10 (a) ($\tan^{-1}(0.33)$ = 18° at z/D = 4.3 at Re = 5000). The reason for this is not clear, but it is possible to assume that the Taylor vortices which may be formed by the centrifugal instability affects the turbulent streaky structure.

In the laminar regime (Figs. 6 and 7), the heat transfer coefficient is almost uniform when the flow is not swirled. And it does not fluctuate over time. In contrast, when the flow is swirled, a streaky structure that inclines in the swirl direction appears. This structure fluctuates over time, which increases the heat transfer. The similar streaky structure was observed at the lower Reynolds number of $Re \approx 1000$ at P/D = 2.5, only in the upstream region.

It is known that when a laminar pipe flow is rotated in the axial direction to swirl the flow, the flow becomes unstable and forms a helical vortex structure (Toplosky and Akylas, 1988;

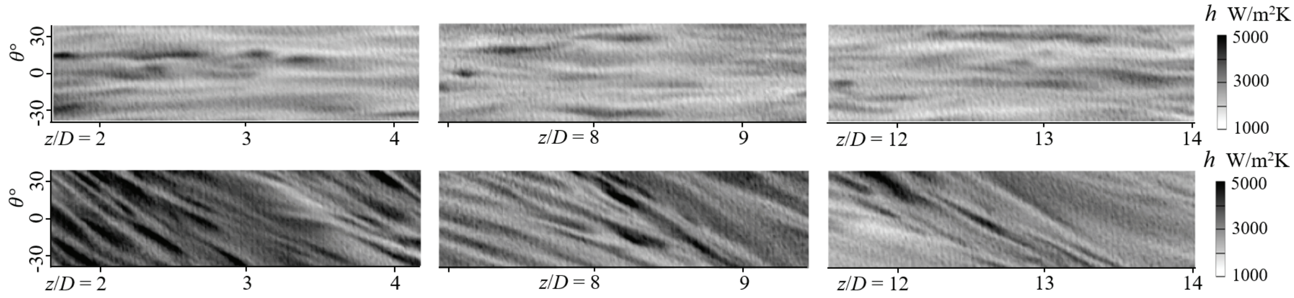

Figure 4. Contours of instantaneous heat transfer coefficient at *Re* = 12000: (a) no swirl (top); (b) *P*/*D* = 2.5 (bottom).

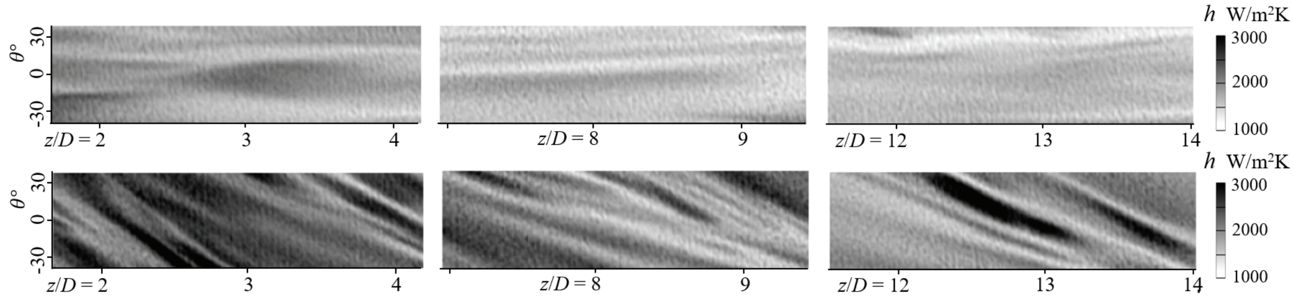

Figure 5. Contours of instantaneous heat transfer coefficient at *Re* = 5800: (a) no swirl (top); (b) *P*/*D* = 2.5 (bottom).

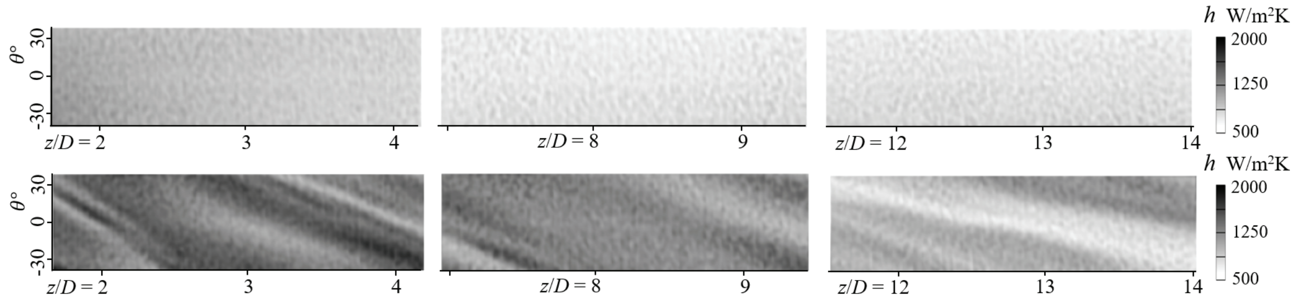

Figure 6. Contour of instantaneous heat transfer coefficient at *Re* = 2200: (a) no swirl (top); (b) *P*/*D* = 2.5 (bottom).

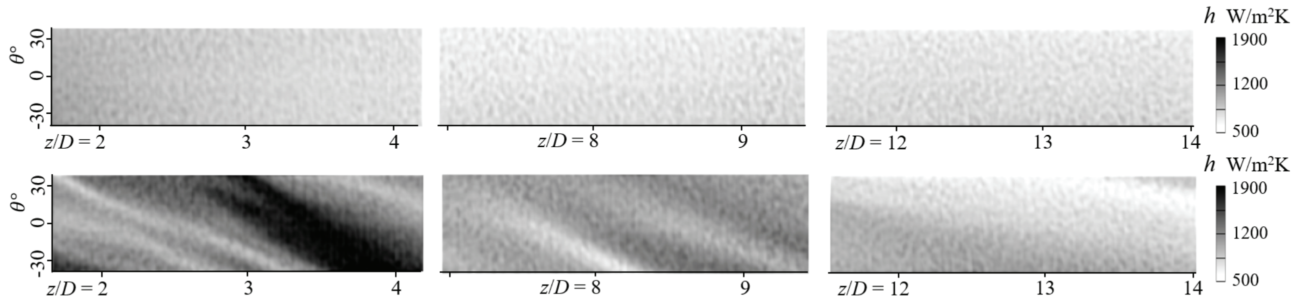

Figure 7. Contour of instantaneous heat transfer coefficient at *Re* =1700: (a) no swirl (top); (b) *P*/*D* = 2.5 (bottom).

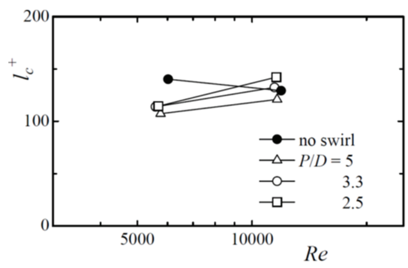

Figure 8. Mean spacing of thermal streaks.

Imao et al. 1992). Similarly, stability analysis of a laminar flow in a pipe shows that the helical wave does not decay and it is sustained when a swirl is applied to the inlet (Landman, 1990). Based on these facts, it is considered that the inclined streaky structure appearing in Figs. 6 (b) and 7 (b) is related to the flow instability due to swirling the laminar pipe flow.

Mean Velocity Field

Figures 9 and 10 show mean streamwise and azimuthal velocities U_z and U_θ, respectively, at *Re* = 5000 (turbulent regime) and *Re* = 1500 (laminar regime). Here, the velocity and length are non-dimensionalized by $2U_m$ and pipe radius *R*.

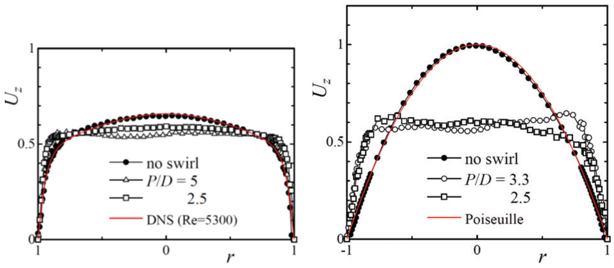

(a) Re = 5000 (b) Re = 1500

Figure 9. Mean streamwise velocity profiles at z/D = 8.3.

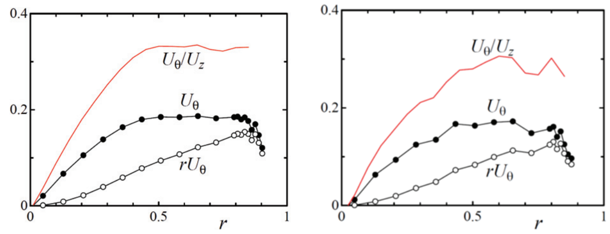

(a) Re = 5000 (b) Re = 2000

Figure 10. Mean azimuthal velocity and angular momentum profiles of P/D = 2.5 at z/D = 4.3.

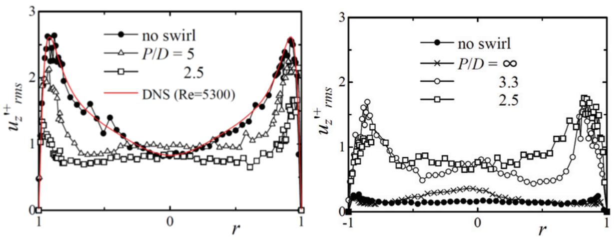

(a) Re = 5000 (b) Re = 1500

Figure 11. Streamwise turbulence intensities $u_z{}'^+_{rms}$ at z/D = 8.3.

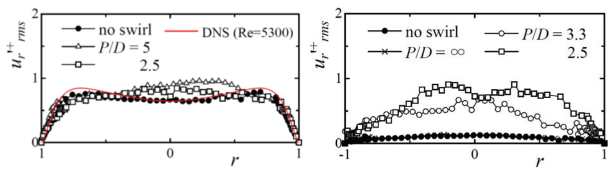

(a) Re = 5000 (b) Re = 1500

Figure 12. Radial turbulence intensities $u_r{}'^+_{rms}$ at z/D = 8.3.

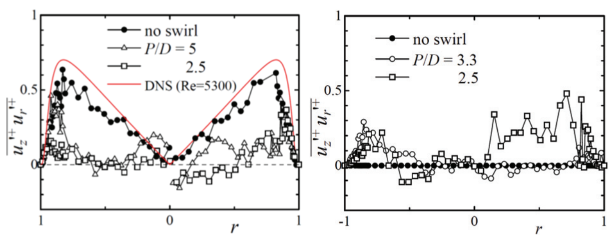

(a) Re = 5000 (b) Re = 1500

Figure 13. Turbulent shear stress $\overline{u_z{}'^+ u_r{}'^+}$ at z/D = 8.3.

In the turbulent regime at Re = 5000, the streamwise velocity in the central part decreases and that near the wall increases when the flow is swirled. This is a general trend by giving the swirl to the turbulent pipe flow (Kreith and Sonju, 1965; Kitoh,

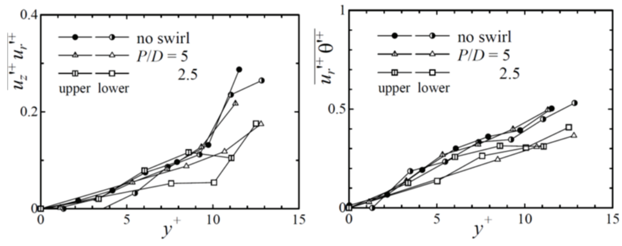

(a) $\overline{u_z{}'^+ u_r{}'^+}$ (b) $\overline{u_r{}'^+ \theta'^+}$ (rough estimate)

Figure 14. Comparison between turbulent shear stress and turbulent heat flux near the wall at z/D = 8.3 at Re = 5000.

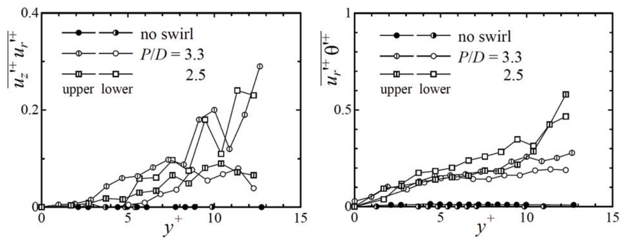

(a) $\overline{u_z{}'^+ u_r{}'^+}$ (b) $\overline{u_r{}'^+ \theta'^+}$ (rough estimate)

Figure 15. Comparison between turbulent shear stress and turbulent heat flux near the wall at z/D = 8.3 at Re = 1500.

1991; Pashtrapanska et al., 2006; among others). For the reference, it is known that the turbulent flow in a rotating pipe shows the opposite trend to approach the Hagen-Poiseuille flow (Kikuyama et al., 1983; Reich and Beer, 1989; Orlandi and Fatica, 1997; among others). This difference can be explained by the following Richardson number, which was derived from the analogy between the buoyancy and centrifugal forces (Bradshaw, 1969; Kikuyama et al., 1983).

$$Ri = \frac{\dfrac{2U_\theta}{r^2}\dfrac{\partial}{\partial r}(rU_\theta)}{\left(\dfrac{\partial U_z}{\partial z}\right)^2 + \left(r\dfrac{\partial}{\partial z}\dfrac{U_\theta}{r}\right)^2} \quad (1)$$

Based on Eq.(1), in the case of $Ri > 0$, that is, when the angular momentum rU_θ increases in the radial direction, the flow is stabilized and the turbulence is suppressed. However, when $Ri < 0$, the flow is destabilized and the turbulence is enhanced. As shown in Fig. 10, for the swirling flow of this experiment, rU_θ increases in the radial direction in the central part ($r < 0.8$), but decreases near the wall ($r > 0.85$). This suggests that the flow is stabilized in the central part but becomes unstable near the wall. This may be related to the smaller streak spacing of $l_c{}^+$ at $Re \approx 5000$. In contrast, in the case of a rotating pipe, Ri number becomes positive in the entire region, resulting in the laminarization of the flow.

In the laminar regime (Fig. 9 (b)), a parabolic velocity distribution of Hagen-Poiseuille flow changes to that similar to the turbulent flow by swirling the flow. This is related to the appearance of the unsteady streaky structure which is considered to be caused by the flow instability due to swirling (Figs. 6 (b) and 7 (b)).

Turbulence distributions

Figures 11 and 12 show turbulent intensities in the streamwise and radial directions $u_z{}'^+_{rms}$ and $u_r{}'^+_{rms}$, respectively. At Re = 5000, both distributions of no swirl are in good agreement with the results of direct numerical simulation (Wu and Moin, 2008, at Re = 5300). By giving the swirl, $u_z'^+_{rms}$ decreases between the wall and central regions (r = 0.5 ~ 0.8), whereas $u_r'^+_{rms}$ hardly changes. The similar trends have been observed in the previous studies (Pashtrapanska et al. 2006; among others). This is likely that there is an energy transfer from the streamwise to other components turbulence between the near wall and the wake region (Chin and Phillip, 2019).

Figure 13 (a) shows turbulent shear stress $\overline{u_z'^+u_r'^+}$ at Re = 5000. It is remarkable that the turbulent shear stress is significantly reduced in the central part (r < 0.8) by swirling the flow. This corresponds to the flow stabilization due to Ri > 0 where the flow is characterized by a forced vortex (Kitoh, 1991). In the near wall region, the turbulent shear stress keeps a relatively large value in the region where Ri < 0. As a whole, the turbulent shear stress is reduced by the flow swirling at Re = 5000, as shown in Fig. 13 (a). Note that $\overline{u_z'^+u_r'^+}$ decreases significantly in the central part (r < 0.5), whereas $u_z'^+_{rms}$ and $u_r'^+_{rms}$ are relatively high. This means that the turbulences in the central region are less correlated each other, and does not contribute much to the turbulent shear stress.

Figure 14 compares the turbulent shear stress $\overline{u_z'^+u_r'^+}$ and the estimated turbulent heat flux $\overline{u_r'^+\theta'^+}$ near the wall at Re = 5000. Here, the non-dimensional fluid temperature is defined by $\theta^+ = (T_m - T)/T_\tau$, where T is fluid temperature and $T_\tau = q_w/(\rho c_p u_\tau)$ is friction temperature. The turbulent heat flux $\overline{u_r'^+\theta'^+} = R_{ur'\theta'}\cdot u_r{}^{+\prime}{}_{rms}\cdot\theta^{+\prime}{}_{rms}$ was estimated using the measured wall temperature fluctuation $T_w'_{rms}$ and the correlation coefficient $R_{ur'\theta'}$ of DNS (Tiselj et al. 2001: turbulent channel flow at Re_τ = 171, constant heat flux, Pr = 5.4). The temperature fluctuation $\theta^{+\prime}{}_{rms}$ was substituted by the measured wall temperature fluctuation based on the fact that the value $\theta^{+\prime}{}_{rms}$ near the wall (y^+ < 13 at $Pr \approx 5$) does not change significantly under a constant heat flux condition. Since there appeared some asymmetry in the flow field when the flow was swirled, the distribution of both the upper and the lower walls were plotted here. As shown in Fig. 14, both the turbulent shear stress and the turbulent heat flux have a similar trend, the value decreases slightly as the flow swirls.

As shown in Fig. 3, the heat transfer increases to the wall shear stress at $Re \approx 5000$. The reason for this is not clear at present, but one of the factors is considered to be the larger decrease in the turbulent shear stress than the turbulent heat flux, as suggested in Fig. 14. This is likely to be due to the significant decrease in the streamwise turbulence $u_z'^+$ compared to the wall-normal turbulence $u_r'^+$. From another point of view, it can be said that the change in the mean streamwise velocity distribution (velocity increase near the wall) due to the swirling (see Fig. 9 (a)) is likely to be a factor of the heat transfer enhancement to the wall shear stress, which can be explained by FIK identity (Kasagi et al. 2012). In any case, the heat transfer enhancement in this regime is considered to be closely related to the change in the vortical structure observed in Figs. 4 and 5, which dominates the momentum and heat transports near the wall.

In the laminar regime at Re = 1500, the turbulence is small in the absence of the twisted tape (no swirl), as shown in Figures 11 (b) and 12 (b) (the turbulence observed here is considered to be mainly due to measurement noise). In addition, measurements were performed with a flat tape without twist (noted as $P/D = \infty$ in the Figures) to investigate the effect of turbulence by the tape insert itself. In this case, the turbulence hardly increases especially near the wall. That is, the disturbance caused by the tape insert itself was small. In contrast, when the swirl is given with the twisted tape, the turbulence intensity approaches the distribution of the turbulent flow. Also, as shown in Fig. 15, the turbulent shear stress and the turbulent heat flux near the wall increase to the similar values as the turbulent flow. Based on these results, it is reasonable to say that the turbulent transition occurs by swirling the flow in the laminar regime. This corresponds to the occurrence of the inclined unsteady streaky structure, as shown in Figs. 6 (b) and 7 (b). According to experiments by García et al. (2012), when the wire coil was installed inside the pipe to swirl the flow, the transition Reynolds number was lower than when other turbulence promoters were installed. This also support the fact that the swirling the laminar flow promotes the turbulent transition.

The heat transfer enhancement against the wall shear stress is often discussed by the ratio of Stanton number to the friction coefficient, St/C_f, derived from the Reynolds analogy. The value St/C_f of the laminar pipe flow for a constant heat flux is $0.27/Pr$, which is derived from $C_f = 16/Re$ and $St = Nu/Re{\cdot}Pr = 4.36/Re{\cdot}Pr$. For the turbulent pipe flow, the value St/C_f can be estimated to $0.5/Pr^{2/3}$ from the Chilton and Colburn j-factor analogy of $St{\cdot}Pr^{2/3} = C_f/2$ in the range Pr = 0.7 ~ 1000 (Chilton and Colburn, 1934). Namely, the parameter St/C_f is generally higher in the turbulent flow than in the laminar flow, especially for the higher Prandtl number. (In the case of Pr = 5, the value St/C_f in the laminar and turbulent regimes are 0.054 and 0.171, respectively.) From this fact, it is fairly certain that the large increase in the heat transfer against the wall shear stress in the laminar regime is caused by the turbulent transition. Accordingly, it can be said that the decrease in the transition Reynolds number due to the flow swirling leads to a large heat transfer enhancement in this regime.

SUMMARY

In this paper, the mechanism of heat transfer enhancement by applying the swirl to an in-pipe flow was considered based on the measurements of spatiotemporal heat transfer and velocity field.

In the turbulent regime, the turbulent shear stress decreased significantly in the central part due to the stabilization by swirling the flow. In contrast, the turbulent shear stress kept a relatively large value in the near wall region, while the non-dimensional streak spacing did not change significantly with the flow swirling. The reason for the heat transfer enhancement in this regime was not clear at present, but one of the factors was considered to be the larger decrease in the turbulent shear stress than the turbulent heat flux near the wall.

In the laminar regime, the decrease in the transition Reynolds number due to the instability by the flow swirling is considered to be the reason for a large heat transfer enhancement. This can be explained by the fact that the parameter St/C_f is generally higher in the turbulent flow than in the laminar flow.

REFERENCES

Bradshaw, P., 1969, "The Analogy Between Streamline Curvature and Buoyancy in Turbulent Shear Flow", *Journal of Fluid Mechanics*, Vol. 36, pp. 177-191.

Chilton, T. H., and Colburn, A. P., 1934, "Mass Transfer (Absorption) Coefficients", *Industrial and Engineering Chemistry*, Vol. 26, pp. 1183-1187.

Chin, R. C., and Philip, J., 2019, "Direct Numerical Simulation of Low Reynolds Number Turbulent Swirling Pipe Flows", *Physical Review Fluids*, Vol. 4, 114607.

Date, A. W., 1974, “Prediction of Fully-Developed Flow in a Tube Containing a Twisted-Tape”, *Int. J. Heat Mass Transf.*, Vol. 17, pp. 845-859.

Eiamsa-ard et al., 2010, “Thermohydraulic Investigation of Turbulent Flow Through a Round Tube Equipped with Twisted Tapes Consisting of Centre Wings and Alternate-Axes”, *Experimental Thermal and Fluid Science*, Vol. 34, pp. 1151–1161.

García, A., Solano, J. P., Vicente, P. G., and Viedma, A., 2012, “The Influence of Artificial Roughness Shape on Heat Transfer Enhancement: Corrugated Tubes, Dimpled Tubes and Wire Coils”, *Applied Thermal Engineering*, Vol. 35, pp. 196-201.

Imao, S., Itoh, M., Yamada, Y., and Zhang, Q., 1992, “The Characteristics of Spiral Waves in an Axially Rotating Pipe”, *Experiments in Fluids*, Vol. 12. pp. 277-285.

Kasagi, N., Hasagawa, Y., Fukagata, K., and Iwamoto, K., Contral of Turbulent Transport: Less Friction and More Heat Transfer”, *ASME J. Heat Transfer*, Vol. 134, 031009.

Kikuyama, K., Murakami, M., and Nishibori, K., 1983, “Development of Three-Dimensional Turbulent Boundary Layer in an Axially Rotating Pipe”, *ASME Journal of Heat Transfer*, Vol. 105, pp. 154-160.

Kitoh, O., 1991, “Experimental Study of Turbulent Swirling Flow in a Straight Pipe”, *Journal of Fluid Mechanics*, Vol. 225, pp. 445-479.

Koch, R., 1960, “Pressure Loss and Heat Transfer for Turbulent Flow”, *United States Atomic Energy Commission, Office of Technical Information*, AEC-tr-3857, Translated from VDI-Forschungsheft, Ser. B. 24, No. 469, 1-44 (1958).

Kreith, F., and Sonju, O. K., 1965, “The decay of a Turbulent Swirl in a Pipe”, *Journal of Fluid Mechanics*, Vol. 22, pp. 257-271.

Landman, M. J., 1990, “On the Generation of Helical Waves in Circular Pipe Flow”, *Physics in Fluids A*, Vol. 2, pp. 738-747.

Lopina, R. F., and Bergles, A. E., 1969, "Heat Transfer and Pressure Drop in Tape-Generated Swirl Flow of Single-Phase Water", *ASME J. Heat Transfer*, Vol. 91, pp. 434-442.

Manglik, R. M., and Bergles, A. E., 1993a, “Heat Transfer and Pressure Drop Correlations for Twisted-Tape Inserts in Isothermal Tubes: Part I – Laminar Flows”, *ASME Journal of Heat Transfer*, Vol. 115, pp. 881-889.

Manglik, R. M., and Bergles, A. E., 1993b, “Heat Transfer and Pressure Drop Correlations for Twisted-Tape Inserts in Isothermal Tubes: Part II – Transition and Turbulent Flows”, *ASME Journal of Heat Transfer*, Vol. 115, pp. 890-896.

Nakamura, H., 2007, “Measurements of Time-Space Distribution of Convective Heat Transfer to Air Using a Thin Conductive-Film”, *5th Int. Symp. on Turbulence and Shear Flow Phenomena*, München, pp. 773-778.

Nakamura, H., Shiibara, N., and Yamada, S., 2017, “Quantitative Measurement of Spatio-Temporal Heat Transfer to a Turbulent Water Pipe Flow”, *Int. J. Heat Fluid Flow*, Vol. 63, pp. 46-55.

Orlandi, P., and Fatica, M., 1997, “Direct Simulations of Turbulent Flow in a Pipe Rotating about Its Axis”, *Journal of Fluid Mechanics*, Vol. 343, pp. 43-72.

Pashtrapanska, M., Jovanovic, J., Lienhart, H, and Durst, F., 2006, “Turbulence Measurements in a Swirling Pipe Flow”, *Experiments in Fluids*, Vol. 41, pp. 813-827.

Reich, G., and Beer, H., 1989, “Fluid Flow and Heat Transfer in an Axially Rotating Pipe – I. Effect of Rotation on Turbulent Pipe Flow”, *Int. J. Heat and Mass Transf.*, Vol. 32, pp. 551-562.

Sheikholeslami, M., Gorji-Bandpy, M., and Ganji, D. D., 2015, “Review of Heat Transfer Enhancement Methods: Focus on Passive Methods Using Swirl Flow Devices”, *Renewable and Sustainable Energy Reviews*, Vol. 49, pp. 444-469.

Tiselj, I., et al., 2001, “Effect of Wall Boundary Condition on Scalar Transfer in a Fully Developed Turbulent Flume”, *Physics of Fluids*, Vol. 13, pp. 1028-1039.

Toplosky, N., and Akylas, T. R., 1988, “Nonlinear Spiral Waves in Rotating Pipe Flow”, *Journal of Fluid Mechanics*, Vol. 190, pp. 39-54.

Wu, X., and Mion, P., 2008, “A Direct Numerical Simulation Study on the Mean Velocity Characteristics in Turbulent Pipe Flow”, *Journal of Fluid Mechanics*, Vol. 606, pp. 81-112.